Available online at www.sciencedirect.com
ScienceDirect
Electrochimica Acta 52 (2007) 2429–2436
ELECTROCHIMICA Acta
www.elsevier.com/locate/electacta

Monte Carlo study of the electrode|solvent primitive model electrolyte interface

S. Lamperski *, A. Zydor

Department of Physical Chemistry, Faculty of Chemistry, A. Mickiewicz University, Grunwaldzka 6, 60-780 Poznań, Poland

Received 12 July 2006; received in revised form 22 August 2006; accepted 23 August 2006
Available online 29 September 2006

Abstract

Results of a Monte Carlo simulation of the electrode|electrolyte interface with and without solvent molecules are reported. The solvent molecules are modelled by neutral hard spheres immersed in a homogeneous dielectric medium. Calculations have been performed for 1:1 and 1:2 electrolytes at $c = 1$ M, with packing fraction $\eta = 0.3$ when the solvent molecules were present, and at a wide range of electrode charge. Insertion of the solvent molecules induces a layering of ion and solvent molecules in the vicinity of the electrode surface. The presence of the solvent molecules reduces the thickness of the electric double layer, lowers the value of the mean electrostatic potential and raises capacitance. The differential capacitance results are compared with the MPB theory predictions.
© 2006 Elsevier Ltd. All rights reserved.

Keywords: Solvent primitive model; Electric double layer; Monte Carlo simulation; Differential capacitance

1. Introduction

The simplest model of the electrode|electrolyte interface, which is even currently used to analyse some anomalous behaviour at low temperatures [1], does not differ too much from that considered by Gouy [2] and Chapman [3]: the only change is that the point charges are replaced by hard spheres with point charges at their centres. The main shortcoming of this model is that the solvent is treated as a continuous medium. Helmholtz [4] was the first to introduce solvent molecules into the model of the electrode|electrolyte interface by assuming ion and electrode solvation. Since then there have been parallel developments of both models and theories which treat the solvent as a medium made up of individual molecules. Different approaches can be found in the literature [5–9]. In the simplest molecular model introduced by Grimson and Rickayzen [10], the solvent molecules are represented by hard spheres immersed in a continuous dielectric medium. This model does not describe the dielectric properties of the interface region, but fairly well characterizes the hard-core interactions. Its importance stems from the fact that it can be used both in molecular simulations and theoretical studies. Thus the theoretical predictions can be directly verified by the simulation results. The model was used in the investigation of phase equilibrium [11], membranes [12,13], ion channels [14], conductivity and diffusivity in a nanopore [15]. We concentrate on its application to the planar electric double layer. In this area, we must mention first of all the comprehensive work of Tang et al. [16]. The authors based their study on density functional theory (DFT). The DFT theory has also been applied by other authors [17–21]. The first reliable but scattered Monte Carlo (MC) results were published by Zhang et al. [22]. Lamperski et al. [23] showed that the modified Poisson–Boltzmann (MPB) extension to solvent molecules was in reasonable agreement with these MC results. The MC investigation of Boda and Henderson [24] revealed anomalous capacitance behaviour at low temperatures. Recently, the influence of the size of the solvent molecules was investigated by di Caprio et al. [25], Stafiej et al. [26] using field theoretical approaches and by Lamperski and Outhwaite [27] using a theory based on incorporating the exclusion volume term into the inhomogeneous Poisson–Boltzmann theory [28,29].

The model which treats solvent molecules as neutral hard spheres is a very simple one and can be used in the analysis of steric effects. More sophisticated models of the solvent like ST2 [30] (Philpott and Glosli [31]) or SPC/E [32] (Schmickler and Leiva [9], Spohr [33,34], Crozier et al. [35]) give much more

* Corresponding author. Tel.: +48 61 8291454; fax: +48 61 8658008.
E-mail address: slamper@amu.edu.pl (S. Lamperski).

0013-4686/$ – see front matter © 2006 Elsevier Ltd. All rights reserved.
doi:10.1016/j.electacta.2006.08.045

realistic description of properties of charged interfaces, but they are too complicated to be described by theory.

In this paper, we present a systematic MC analysis of the steric effect imposed by the solvent molecules on the properties of the electrode|electrolyte interface. Additionally, we describe a new procedure for calculating the differential capacitance from the MC results and compare the capacitance results with the predictions of MPB theory [36] and its extension to solvent molecules [23]. The structure of the paper is similar to that of Tang et al. [16]. However, as our intention is not to assess the results of these authors but to give reliable MC results useful for comparison with the theoretical predictions, we use slightly different molecular parameters and consider a 1:2 rather than a 2:2 electrolyte. The behaviour of the divalent counter-ions of 2:2 and 1:2 electrolytes at the interfacial region is similar [37] but the 1:2 electrolyte reveals some additional interesting features at small electrode charges due to the charge asymmetry of ions.

2. Model

The electrode|electrolyte interface occurs when an electrolyte is in contact with the charged surface of a metal (electrode). We assume that the electrode is a planar, infinitely large hard wall carrying a uniform electrical surface charge, σ. The electrolyte is composed of ions and solvent molecules. The ions are represented by hard spheres of diameter d with the electric charge ze embedded at the centre (e is the elementary charge and z its charge number). The solvent molecules are neutral hard spheres having the same diameter as the ions. All the species are immersed in a homogeneous medium of relative electrical permittivity, ε_r. Its value is typical of the considered solvent. Thus the properties of the solvent are described by two parameters: molecular d and thermodynamic ε_r. Such a model is called the solvent primitive model (SPM). The results from the SPM theory are compared with those of the restricted primitive model (RPM) of the electrolyte. The word 'restricted' means that the diameters of anions and cations are the same. In the RPM, the solvent is represented by a continuous medium of permittivity ε_r.

3. Simulation details

The simulations were performed using the standard Metropolis canonical Monte Carlo technique, similar to that applied by Torrie and Valleau [38]. The simulation box was a rectangular prism of size $W \times W \times L$. Two opposite, square walls of the side length W represented the electrodes while the distance between the electrodes was L. The electrode was characterized by the electrical surface charge σ. For the symmetrical 1:1 electrolyte only one electrode was charged (the opposite electrode was discharged) while the asymmetrical 1:2 electrolyte required two charged electrodes. When simulating the asymmetrical electrolyte in the box with one charged electrode the anion and cation distribution functions deviate in the vicinity of the discharged electrode. This leads to electrical charge being concentrated near the discharged electrode. This charge disturbs the results. The electrodes are impenetrable to ions, so the periodic boundary conditions and the minimum image convention were applied to the directions parallel to the electrode surface. The simulation box contained N_- anions, N_+ cations and optionally N_0 solvent molecules. The numbers N_- and N_+ together with L and W have to fulfil two conditions: give the required bulk molar ion concentrations c_-, c_+ and the desired surface charge, σ

$$\sigma = \frac{-e(z_- N_- + z_+ N_+)}{n_e W^2}, \tag{1}$$

where n_e is the number of charged electrodes of the simulation box ($n_e = 1$ for the 1:1 electrolyte and $n_e = 2$ for 1:2 one). Additionally, the numbers of all the species have to give the assumed bulk packing fraction, η

$$\eta = \frac{\pi d^3(\rho_-^o + \rho_+^o + \rho_0^o)}{6}. \tag{2}$$

Here ρ_i^o is the bulk density number of species i. We have assumed that when the solvent molecules are present, the packing fraction η of the 1:1 and 1:2 electrolyte is equal to 0.3. This value is slightly lower than that used by Tang et al. [16] ($\eta_{solv} \approx 0.3665$) or Patra and Ghosh [20] ($\eta_{solv} \approx 0.4189$). However at higher η non-ergodicity could occur. This is characteristic for a hard sphere fluid at high density [39]. Due to non-ergodicity the precision of the MC results decreases. We expect that the applied concentration of solvent is sufficiently low to avoid the ergodicity problem and high enough to observe and analyse the result of steric effect imposed by the hard sphere solvent molecules.

The electrostatic and/or hard-core overlap interactions between all the particles located in the simulation box, and between these particles and the electrodes, were calculated explicitly. To estimate the long-range electrostatic interactions the method of infinitely large, equidistantly spaced, charged planes with a square hole for the simulation box was used [38]. The Verlet neighbour list [40] was applied to facilitate the computations when the solvent molecules were present.

The simulations were performed for the electrode charges, σ/C m^{-2}, changing from -0.1 to $+1.0$. We assumed that the bulk concentration of both 1:1 and 1:2 (divalent anion) electrolytes was equal to 1 M, with $\varepsilon_r = 78.5$, $d = 400$ pm, $T = 298.15$ K, $W = 4902.316$ or 5063.196 pm, and $L \approx 8100$ pm for two charged electrodes or approximately 4800 pm for one charged electrode. The required bulk concentrations were obtained by small adjustments to the box length, L, or to the number of ions, N_-, N_+, and/or to the solvent molecules, N_0. The value of d assumed in the calculations needs a comment. It is approximately the mean crystallographic diameter of simple spherical anions: Cl^- (362 pm), Br^- (392 pm) and I^- (440 pm) [41]. Other authors used 425 pm [38] or 300 pm [42] for the ion diameter.

To equilibrate the SPM system we used 150×10^6 (30×10^6 for RPM) MC configurations. The averages were calculated from the next 300×10^6 configurations (60×10^6 for RPM). Simulations for RPM were repeated three times at each σ to improve the statistics. Such a procedure was not sufficient for SPM. Here, at each σ we repeated the simulations until obtaining five sets of results with a flat ion and solvent distribution in the central part of the simulation box. The average of these sets was taken for further analysis.

The main average quantity obtained from the simulation was the concentration distribution of each species against the electrode surface described by the singlet distribution function, $g_i(x)$. It was calculated as a local density $\rho_i(x)$ at a distance x from the electrode surface related to the bulk density, ρ_i^o:

$$g_i(x) = \frac{\rho_i(x)}{\rho_i^o}, \quad i = -, +, 0. \tag{3}$$

The contact value of the distribution function, $g_i(d/2)$, was obtained by a polynomial extrapolation. The bulk density was obtained by averaging the density profile in its flat region (the bulk molarity, $c_i = \rho_i^o/1000N_A$, N_A is the Avogadro constant). The singlet distribution function was used to calculate the mean electrostatic potential

$$\psi(x) = -\frac{e}{\varepsilon_r\varepsilon_0}\sum_{i=-,+} z_i\rho_i^o \int_{\max(x,d/2)}^{\text{flat region}} g_i(x_1)(x_1 - x)\,\mathrm{d}x_1. \tag{4}$$

Here ε_0 is the electrical permittivity of vacuum. From the potential of the electrode, $\psi(0)$, the integral capacitance, C_{int}, was calculated

$$C_{\text{int}} = \frac{\sigma}{\psi(0)}. \tag{5}$$

The differential capacitance, C_{diff}, of the interface

$$C_{\text{diff}} = \frac{\mathrm{d}\sigma}{\mathrm{d}\psi(0)} \tag{6}$$

is the main, experimentally available quantity. Its calculation from the MC results requires application of numerical differentiation. However, our results are not smooth enough to perform a standard three point $[y'_n = (y_{n+1} - y_{n-1})/2h]$ or a more precise five point $[y'_n = (-y_{n+2} + 8y_{n+1} - 8y_{n-1} + y_{n-2})/12h]$ numerical differentiation. It is well known that numerical differentiation amplifies roughness. Also the analytical form for the $\psi(0) - \sigma$ dependence, which would be useful in our studies, is unknown. To our best knowledge, there is no information in literature on calculation of differential capacitance of the electric double layer from MC results. Therefore, to carry out such calculations we elaborated and applied the following algorithm. Let the points (σ, $\psi(0)$) be arranged in order of increasing surface charge. The nth degree polynomial ($n \leq 3$) is fitted to the first five points by the least square method. Such an interpolation polynomial smoothes out the results without losing their physical meaning. The derivative of the polynomial is calculated for the first three points. Its inverse is the differential capacitance. The algorithm is repeated for the consecutive five points starting from the second one, but now the capacitance is calculated for the middle point, only. The calculations are continued until the last five points are reached. Then the capacitance is calculated for the last three points. The algorithm works pretty-well (see Figs. 9 and 10), but it must be realised that the precision of the differential capacitance for the first and the last two points is lower than for the central points. Further in the text we will call this algorithm the *interpolation polynomials method*.

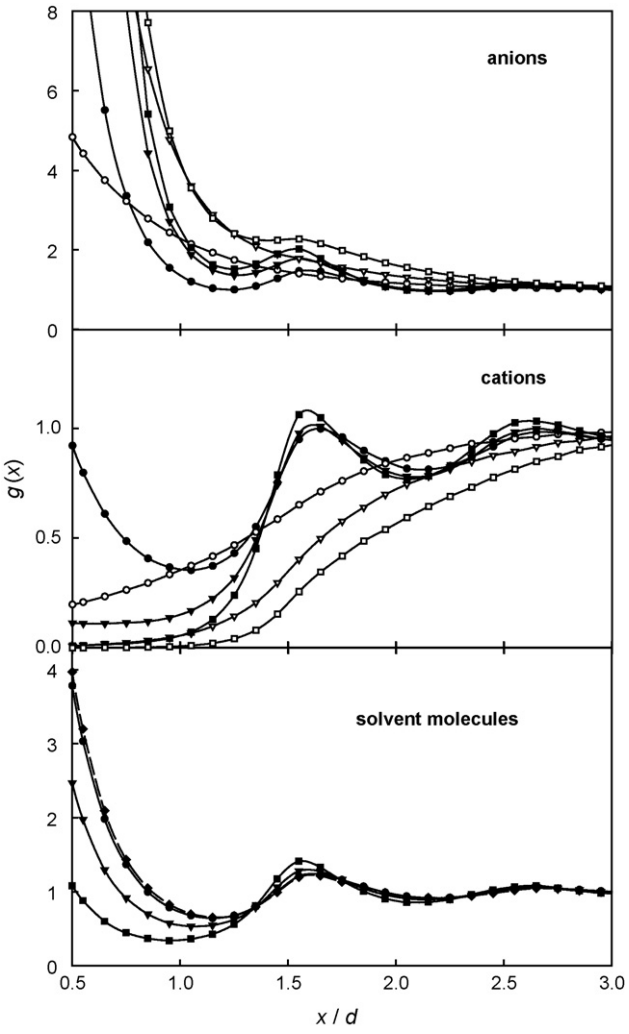

Fig. 1. Singlet distribution functions of anions, cations and solvent molecules for a 1:1 electrolyte at σ/C m^{-2} = 0.1 (circles), 0.3 (triangles) and 0.5 (squares). The solid symbols correspond to the system with SPM while the open symbols to RPM. The dashed line with diamonds corresponds to the discharged system at η = 0.3. The other parameters as in the text.

4. Results and discussion

We begin the discussion by considering the singlet distribution functions. These functions provide information about the structure of the electrolyte in the vicinity of the electrode surface and are used to calculate the thermodynamic properties of the interfacial region. In Fig. 1, we show separately the distribution functions of anions, cations and solvent molecules for a 1:1 electrolyte at σ/C m^{-2} = 0.1 (circles), 0.3 (triangles) and 0.5 (squares). The open graphic symbols correspond to RPM while the solid to the SPM electrolyte. The MC points have been joined by lines to guide the eye. The singlet distribution functions for a 1:1 RPM electrolyte at relatively small electrode charges are similar to those predicted by the Gouy–Chapman–Stern (GCS) theory [2,3,43]: the positively charged electrode attracts anions and repels cations. At higher electrode charges, an additional peak appears on the anion distribution curve at $x/d \approx 1.55$. This is due to the formation of a second layer of anions (the counter-

ion layering effect) [28,29]. Insertion of the neutral hard spheres reduces the amount of free volume and thus the molecules form more structured configurations. In the vicinity of the planar electrode surface damped oscillations in the concentration distributions take place. This effect for discharged inhomogeneous system (the hard wall and the hard spheres) at $\eta = 0.3$ is shown in the bottom sub-figure of Fig. 1 by the dashed line with diamonds. The oscillations imply a layering of the solvent molecules in the vicinity of the electrode surface which influence the distribution of the ions. The maximum of the singlet distribution function of anions at the contact distance ($x/d = 0.5$) is higher and thinner than that for the system without solvent molecules. Also, new maxima are observed at $x/d \approx 1.55$ and 2.65. The cation distribution curves exhibit the analogous new maxima. An interesting behaviour of the cations is observed in the immediate vicinity of the electrode surface. Here, we have a competition between electrostatic and steric forces. The electric charge of the electrode repels the cations, while the solvent molecules support their adsorption. The qualitatively similar behaviour of the cations in the vicinity of the electrode was predicted by the DFT [16,20] and MPB [23] theories and also by the earlier MC simulation [22,24]. Consideration of the realistic model of water changes this picture. Spohr [33] found that e.g. near the uncharged electrode surface the concentration of Cl^- ions is significantly reduced, while the concentration of water molecules at the same distance is large. This is perhaps due to the anion solvation. The solvation effect cannot be observed for SPM, as there is no attraction term in the ion–solvent potential. Generally, any comparison of our results with those of the realistic model of ions and solvent molecules is difficult because of the different size of the species in the realistic model. Also the hard-core interactions are soft. This makes that the density oscillations are not as strong as for the SPM model.

Hitherto, we have discussed the influence of the solvent molecules on the ion distribution. But the reverse effect also exists. The adsorption of the anions leads to the depletion of solvent molecules, which is evidenced by the distribution functions of solvent molecules. The removed solvent molecules concentrate at some greater distance contributing to the peak at $x/d \approx 1.55\,d$. The same behaviour is observed for the charge dependence of the exclusion volume term, this term describing the distribution of the uncharged ion of species α at a charged interface. The exclusion volume term plays an important role in the theory of charged systems [36].

In Fig. 2, we present the singlet distribution functions for the 1:2 electrolyte. The RPM curves exhibit a different behaviour than those for 1:1 electrolyte and the predictions of the GCS theory are completely unsatisfactory here [29,44]. However, more sophisticated theories such as a density functional [16,21,42] or a MPB theory [45] provide a correct description the ion distribution of 1:2 RPM electrolyte interface. As shown in Fig. 2, the solvent molecules alter the ion distribution in a similar way as observed for the 1:1 electrolyte. It is worth noting that the depletion of the solvent molecules from the vicinity of the electrode is weaker than that discussed previously. The explanation of this phenomenon is as follows. At the same electrode charge the number of divalent anions is approximately two times lower

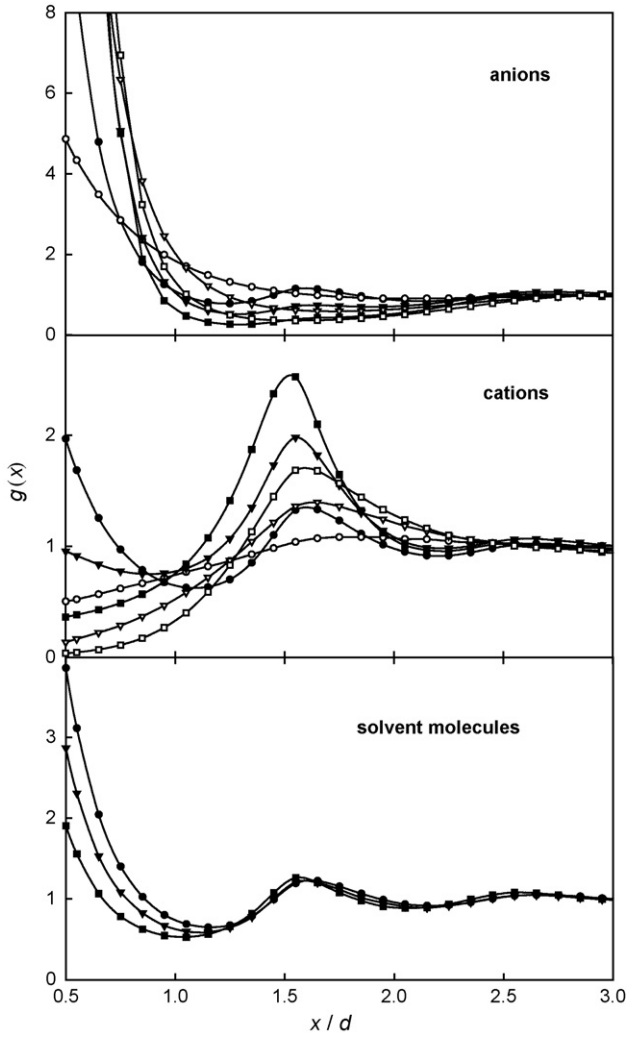

Fig. 2. Singlet distribution functions of anions, cations and solvent molecules for a 1:2 electrolyte at $\sigma/\mathrm{C\,m^{-2}} = 0.1$, 0.3 and 0.5. The symbols have the same meaning as in Fig. 1.

than that of the monovalent ones. Thus, the steric repulsion of the solvent molecules by the adsorbed divalent anions is weaker in this case.

Integration of the singlet distribution function gives, according to Eq. (4), the mean electrostatic potential. The results for the 1:1 and 1:2 electrolytes are shown in Figs. 3 and 4, respectively. For the 1:1 electrolyte, we observe a monotonic exponential-like decay of the mean potential. At large distances, the potential tends to zero. The curves for SPM lie below the corresponding RPM curves. The separation between the curves increases with increasing electrode charge. The situation is different for the 1:2 electrolyte. Here, the mean potential curves have a negative minimum value at $x/d \approx 0.6$, and then the curves gradually tend to zero at larger x values. Again the presence of solvent molecules generally lowers the value of the mean electrostatic potential. However, in some region after the minimum the potential of the SPM electrolyte is higher than that of the RPM.

Dependence of the mean electrostatic potential at the contact distance, $\psi(d/2)$, called the diffuse layer potential, against the electrode surface charge is regarded as the equation of state for

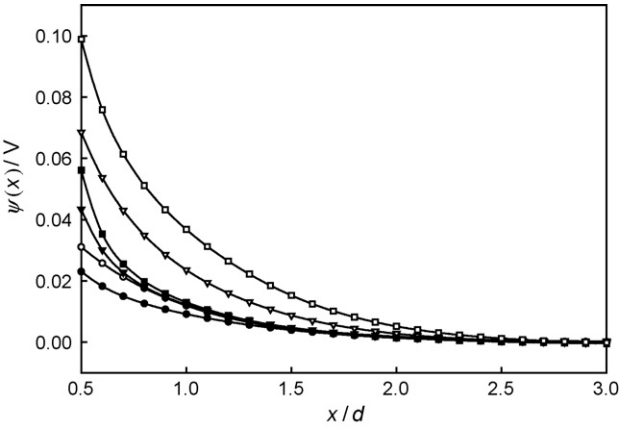

Fig. 3. The profile of mean electrostatic potential for a 1:1 electrolyte at σ/C m^{-2} = 0.1, 0.3 and 0.5. The symbols have the same meaning as in Fig. 1.

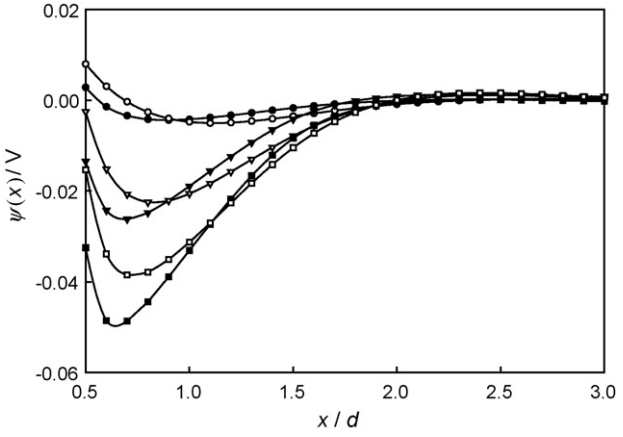

Fig. 4. The profile of mean electrostatic potential for a 1:2 electrolyte at σ/C m^{-2} = 0.1, 0.3 and 0.5. The symbols have the same meaning as in Fig. 1.

charged inhomogeneous systems. We present this dependence for the 1:1 and 1:2 electrolytes in Figs. 5 and 6, respectively. For the 1:1 electrolyte we observe a monotonic increase of the diffuse layer potential in the whole range of electrode charges. The

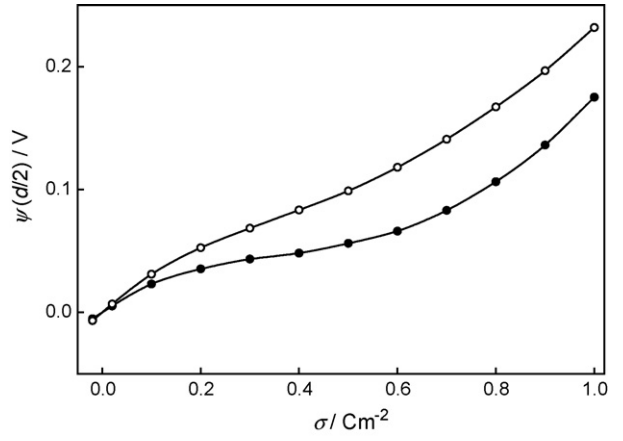

Fig. 5. Mean electrostatic potential at the contact distance $\psi(d/2)$ as a function of the surface charge density for a 1:1 electrolyte. The solid circles correspond to the system with SPM while the open circles to RPM.

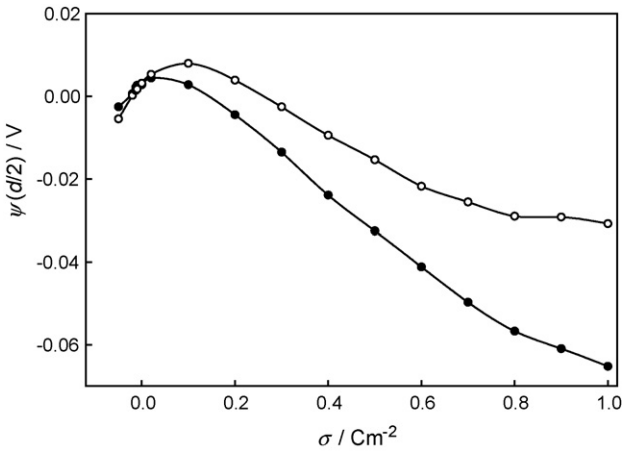

Fig. 6. Mean electrostatic potential at the contact distance $\psi(d/2)$ as a function of the surface charge density for a 1:2 electrolyte. The symbols have the same meaning as in Fig. 5.

behaviour of the 1:2 electrolyte is different. The curves resemble an inverted parabola with a maximum at low, positive electrode charges. The potential reaches positive values only in the vicinity of the maximum. At higher electrode charges the potential is negative. This sign change is characteristic for strong electrostatic interactions. That is why it is observed for divalent counter-ions [42,44,45] and presumably for low electrical permittivity solvents [37]. It occurs also at high electrolyte concentrations [38]. The presence of the solvent molecules causes a decrease in the value of the diffuse layer potential, which means that they reduce the thickness of the diffuse layer. The influence of the solvent molecules on the potential is smaller than that predicted by Tang et al. [16], presumably because we assumed a lower density of the solvent molecules.

The electrode potential, $\psi(0)$, is a sum of the potential drop across the inner layer (here it is the range between the electrode surface and the contact distance) and the potential of the diffuse layer

$$\psi(0) = \sigma d/2\varepsilon_0\varepsilon_r + \psi(d/2). \quad (7)$$

The first term comprises the information about the thickness of the inner layer (d/2) and the electric field ($\sigma/\varepsilon_0\varepsilon_r$) occurring in this region. Its value is usually several times higher than that of the second term. So the dependence of the electrode potential against the electrode surface charge shown in Figs. 7 and 8 for 1:1 and 1:2 electrolytes, respectively, is nearly linear with a positive slope. In both cases, the curve for the SPM electrolyte lies below the corresponding RPM curve. The curves for the 1:1 electrolyte cross the σ axis exactly at the origin of the coordination system while for the 1:2 case—at small negative electrode charges (at σ_0/C m^{-2} ≈ −0.0092 for SPM and −0.0074 for RPM). The electrode potential at σ = 0 amounts to 0.0028 V for SPM and 0.0032 V for the RPM electrolyte. This phenomenon is due to the charge asymmetry of the ions [37].

The charge dependence of the integral capacitance, C_{int}, calculated from the electrode potential results is shown in Figs. 9 and 10 by graphic characters (solid circles—SPM, open circles—RPM). The dashed lines show the integral capacitance

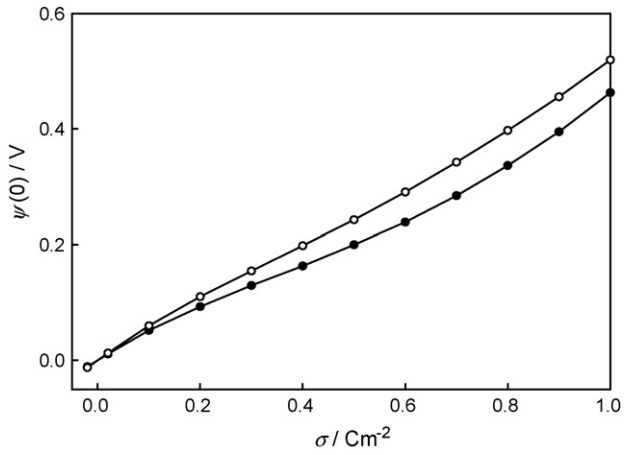

Fig. 7. Electrostatic potential of the electrode $\psi(0)$ as a function of the surface charge density for a 1:1 electrolyte. The symbols have the same meaning as in Fig. 5.

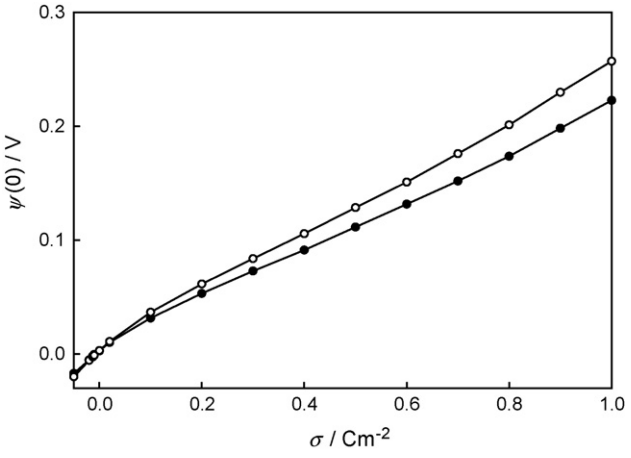

Fig. 8. Electrostatic potential of the electrode $\psi(0)$ as a function of the surface charge density for a 1:2 electrolyte. The symbols have the same meaning as in Fig. 5.

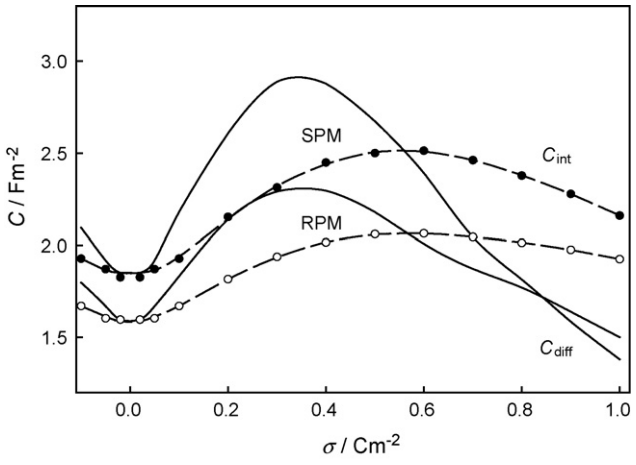

Fig. 9. Capacitance of the electrical double layer as a function of the surface charge density for a 1:1 electrolyte (MC integral capacitance: solid circles—SPM, open circles—RPM; from the interpolation polynomials method: integral capacitance—dashed lines, differential capacitance—solid lines).

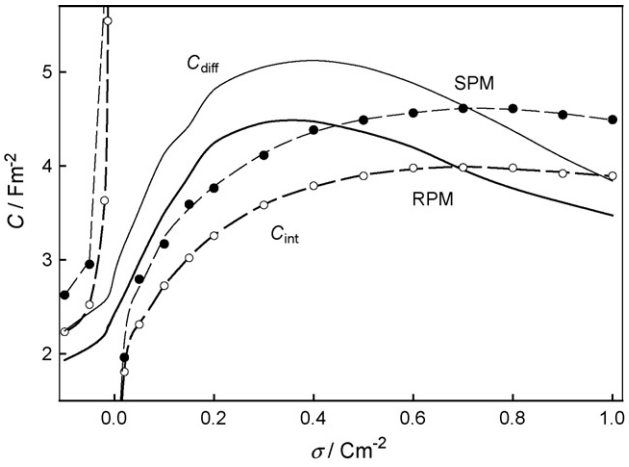

Fig. 10. Capacitance of the electrical double layer as a function of the surface charge density for a 1:2 electrolyte. Notation as Fig. 9.

calculated from the potential obtained from the *interpolation polynomials method* described in the previous section. The curves are very well fitted to the graphic symbols, which permits expecting that the differential capacitance results from the interpolation polynomial are also correct.

The presence of the solvent molecules increases the integral capacitance of both 1:1 and 1:2 electrolytes (see also Ref. [24]). This confirms our earlier opinion that the insertion of the solvent molecules reduces the thickness of the interfacial region. The capacitance curves for 1:1 electrolyte (Fig. 9) have a well-defined maximum at $\sigma/\mathrm{C\,m^{-2}} \approx 0.6$. Here, the separation of the SPM and RPM curves is the largest. The decrease in the capacitance after the maximum is a result of formation of the second layer of anions. This increases the thickness of the interfacial region. The shape of the capacitance curve for 1:2 electrolyte is different. The maximum is flat and the decrease in the capacitance after the maximum is small. It means that at very high electrode charge, varying the charge has only a small influence on the thickness of the interfacial region. The plot of the integral capacitance against the electrode charge is discontinuous at σ_0 because of the zero potential at this charge.

The dependence of the differential capacitance, C_{diff}, on the electrode charge calculated from the *interpolation polynomials method* is shown in Figs. 9 and 10 by solid lines for 1:1 and 1:2 electrolytes, respectively. We used the third order polynomials for the 1:1 electrolyte and the second order ones for the 1:2 electrolyte. As one can expect, for a symmetrical 1:1 electrolyte at $\sigma = 0$ the integral and differential capacitances have the same value (Fig. 9), but with increasing σ the differential capacitance rises faster than the integral one, and reaches a maximum at lower electrode charges, at $\sigma/\mathrm{C\,m^{-2}} \approx 0.35$. The SPM curve goes above the RPM one. A different behaviour is observed only at very high electrode charges, above $0.8\,\mathrm{C/m^2}$. The differential capacitance curves for a 1:2 electrolyte do not exhibit discontinuity observed for the integral capacitance at $\psi(0) = 0$. They have a well formed maximum at $\sigma/\mathrm{C\,m^{-2}} \approx 0.35$ (RPM) and 0.4 (SPM). The SPM curve goes above the RPM one in the whole range of the investigated electrode charges. Our C_{diff} results for 1:1 RPM and SPM as well as for 1:2 RPM electrolyte coincide

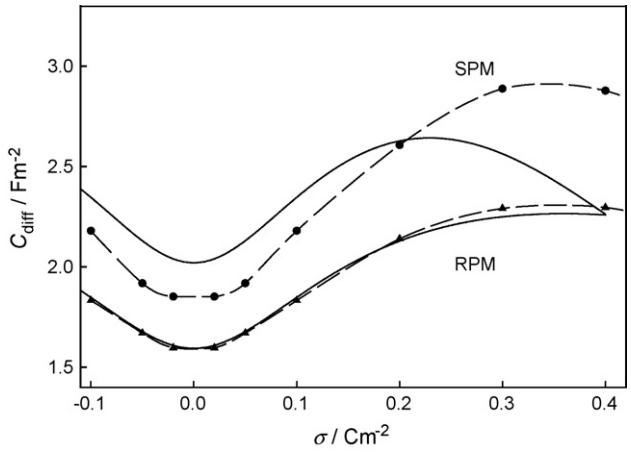

Fig. 11. Differential capacitance of the electrical double layer as a function of the surface charge density for a 1:1 electrolyte calculated from the MPB theory (solid lines) and from the interpolation polynomials method (dashed lines with graphic characters: solid circles—SPM, open circles—RPM).

well with the DFT predictions of Tang et al. [16]. Some differences are observed for 1:2 SPM case. Tang et al. [16] found that the capacitance maximum occurs at higher electrode charges and the value at the maximum is approximately two times higher than our.

We compare in this paper the differential capacity results of the MPB theory [36] and its extension to SPM [23] with our MC data, both calculated for exactly the same values of the physical parameters. The comparison is presented in Figs. 11 and 12 for 1:1 and 1:2 electrolytes, respectively. Solid line shows the MPB predictions. A comparison with Figs. 9 and 10 shows that the range of the electrode surface charge is limited here to 0.4 C/m^2 for a 1:1 electrolyte and to 0.2 C/m^2 for a 1:2 one. This is due to some numerical problems arriving when solving the MPB theory at higher electrode charges. The quantitative agreement for 1:1 RPM electrolyte is excellent, as noticed earlier e.g. by Carnie and Torrie in their review paper [37]. This agreement becomes a little-bit worse when increasing counter-ion charge or adding solvent molecules. The MPB theory predicts higher capacitance at small electrode charges and a maximum located at lower charges. Nevertheless, the qualitative agreement is still satisfactory.

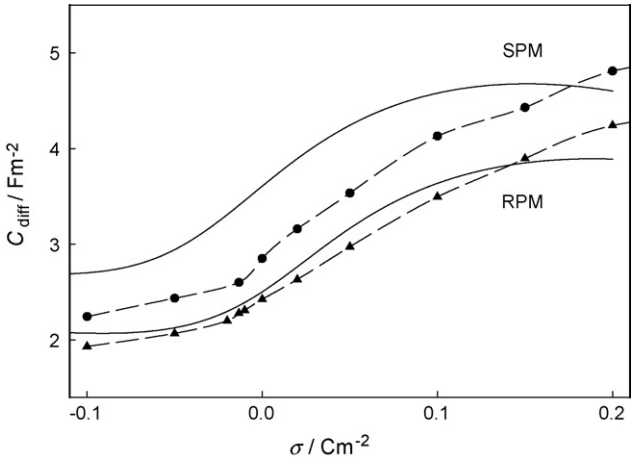

Fig. 12. Differential capacitance of the electrical double layer as a function of the surface charge density for a 1:2 electrolyte calculated from the MPB theory and from the interpolation polynomials method. Notation as Fig. 11.

5. Conclusions

The conclusions following from our results confirm the DFT predictions of Tang et al. [16]. Insertion of neutral hard spheres, representing solvent molecules, induces the layering of ions and solvent molecules in the vicinity of the planar electrode surface. Presence of the solvent molecules reduces the thickness of the electric double layer, lowers the value of the mean electrostatic potential and increases the integral and differential capacitance. We performed simulations at bulk packing fraction values lower than those considered by Tang et al. [16] and Patra and Ghosh [20]. Because of this, we observed less pronounced damped oscillatory distributions of the ions and the solvent molecules. Also the changes we observed in the electrostatic potential and electrical capacitance were smaller. On the other hand, the use of lower concentrations of the solvent molecules allowed us to obtain comparatively precise results.

The MC results presented in this paper can be used to asses usefulness of a particular theory describing properties of the electrode|SPM electrolyte interface. We have compared the MC differential capacitance results with the theoretical MPB predictions and found a good qualitative agreement, better for the 1:1 electrolyte.

The MC simulations of SPM in the canonical ensemble are difficult not only because of the high packing fraction but also due to the small adjustments to the box length or to the number of ions and solvent molecules needed to obtain the required bulk concentrations. These difficulties could be solved by application of the grand canonical Monte Carlo technique. Lee et al. [46] used this technique to investigate forces between charged surfaces in an electrolyte with SPM. They were able to perform simulations even at one order lower bulk electrolyte concentration (0.1 M) and at a similar packing fraction of the solvent ($\eta_{solv} = 0.3$). Thus, it seems that this technique can be useful also in investigation of the electrode|SPM interfaces at low electrolyte concentrations.

Acknowledgements

We are very grateful to Professor C.W. Outhwaite, University of Sheffield, and Professor L.B. Bhuiyan, University of Puerto Rico, for their comments and suggestions. Financial support from Adam Mickiewicz University, Faculty of Chemistry, is appreciated.

References

[1] J. Resko-Zygmunt, S. Sokołowski, D. Henderson, D. Boda, J. Chem. Phys. 122 (2005) 084504.
[2] G. Gouy, J. Phys. (Paris) 9 (1910) 457.
[3] D.L. Chapman, Philos. Magn. 25 (1913) 475.
[4] H. Helmholtz, Ann. Physik. 7 (1879) 337.
[5] R.J. Watts-Tobin, Philos. Magn. 61 (1961) 133.
[6] M. Molero, C.W. Outhwaite, J. Chem. Soc. Faraday Trans. 86 (1990) 35.

[7] S. Lamperski, C.W. Outhwaite, J. Electroanal. Chem. 460 (1999) 135.
[8] G.M. Torrie, P.G. Kusalik, G.M. Patey, J. Chem. Phys. 90 (1989) 4513.
[9] W. Schmickler, E. Leiva, Mol. Phys. 86 (1995) 737.
[10] M.J. Grimson, G. Rickayzen, Chem. Phys. Lett. 86 (1982) 71.
[11] T. Kristof, D. Boda, I. Szalai, J. Chem. Phys. 113 (2000) 7488.
[12] D. Boda, D. Henderson, A. Patrkiejew, S. Sokołowski, J. Chem. Phys. 113 (2000) 802.
[13] D. Boda, D. Henderson, A. Patrkiejew, S. Sokołowski, J. Colloid Interface Sci. 239 (2001) 432.
[14] D. Gillespie, W. Nonner, R.S. Eisenberg, J. Phys. Condens. Matter 14 (2002) 12129.
[15] Y.W. Tang, I. Szalai, K.Y. Chan, J. Phys. Chem. A 105 (2001) 9616.
[16] Z. Tang, L.E. Scriven, H.T. Davis, J. Chem. Phys. 97 (1992) 494.
[17] R.D. Groot, Phys. Rev. A 37 (1988) 3456.
[18] R.D. Groot, J.P. Van der Eerden, J. Electroanal. Chem. 247 (1988) 73.
[19] C.N. Patra, S.K. Ghosh, Phys. Rev. E 48 (1993) 1154.
[20] C.N. Patra, S.K. Ghosh, J. Chem. Phys. 100 (1994) 5219.
[21] C.N. Patra, S.K. Ghosh, J. Chem. Phys. 101 (1994) 4143.
[22] L. Zhang, H.T. Davis, H.S. White, J. Chem. Phys. 98 (1993) 5793.
[23] S. Lamperski, C.W. Outhwaite, L.B. Bhuiyan, Mol. Phys. 87 (1996) 1049.
[24] D. Boda, D. Henderson, J. Chem. Phys. 112 (2000) 8934.
[25] D. di Caprio, Z. Borkowska, J. Stafiej, J. Electroanal. Chem. 540 (2003) 17.
[26] J. Stafiej, A. Ekoka, Z. Borkowska, J.P. Badiali, J. Chem. Soc. Faraday Trans. 92 (1996) 3677.
[27] S. Lamperski, C.W. Outhwaite, J. Electroanal. Chem. 567 (2004) 263.
[28] S. Lamperski, C.W. Outhwaite, Langmuir 18 (2002) 3423.
[29] S. Lamperski, L.B. Bhuiyan, J. Electroanal. Chem. 540 (2003) 79.
[30] F.H. Stillinger, A. Rahman, J. Chem. Phys. 60 (1974) 1545.
[31] M.R. Philpott, J.N. Glosli, J. Electrochem. Soc. 142 (1995) L25.
[32] H.J. Berendsen, J.R. Grigera, T.P. Straatsman, J. Phys. Chem. 91 (1987) 6269.
[33] E. Spohr, J. Electroanal. Chem. 450 (1998) 327.
[34] E. Spohr, Electrochim. Acta 44 (1999) 1697.
[35] P.S. Crozier, R.L. Rowley, D. Henderson, J. Chem. Phys. 114 (2001) 7513.
[36] C.W. Outhwaite, L.B. Bhuiyan, J. Chem. Soc. Faraday Trans. 2 79 (1983) 707.
[37] S.L. Carnie, G.M. Torrie, Adv. Chem. Phys. 56 (1984) 141.
[38] G.M. Torrie, J.P. Valleau, J. Chem. Phys. 73 (1980) 5807.
[39] D.W. Heermann, Computer Simulation Methods in Theoretical Physics, second ed., Springer–Verlag, Berlin/Heidelberg, 1990, p. 71 (Chapter 4).
[40] M.P. Allen, D.J. Tildsley, Computer Simulation of Liquids, Claredon Press, Oxford, 1987, p. 147 (Chapter 5).
[41] R.D. Shanon, C.T. Prewitt, Acta Cryst. B25 (1969) 925.
[42] D. Boda, W.R. Fawcett, D. Henderson, S. Sokołowski, J. Chem. Phys. 116 (2002) 7170.
[43] O.Z. Stern, Electrochemistry 30 (1924) 508.
[44] G.M. Torrie, J.P. Valleau, J. Phys. Chem. 86 (1982) 3251.
[45] L.B. Bhuiyan, C.W. Outhwaite, Phys. Chem. Chem. Phys. 6 (2004) 3467.
[46] M. Lee, K.Y. Chan, Y.W. Tang, Mol. Phys. 100 (2002) 2201.